Antenna System Combining Sensing and Communication Tasks for Cognitive Radio Front-Ends

HAMZA NACHOUANE[1], ABDELLAH NAJID[1], ABDELWAHED TRIBAK[1], FATIMA RIOUCH[1], ANGEL MEDIAVILLA[2]
[1]National Institute of Posts and Telecommunications, Rabat, MOROCCO.
[2]DICOM, University of Cantabria, Santander, SPAIN.
{nachouane,najid,tribak,riouch}@inpt.ac.ma
angel.mediavilla@unican.es

Abstract: - This paper presents an antenna system combining sensing and communication tasks, to be implemented into the RF front-end for cognitive radio systems. The sensing task was performed by the means of an ultra-wideband quasi-omnidirectional antenna. Whilst, the communication task was ensured by a narrowband antenna. Both antennas were designed on the same layer of a FR4 substrate. Therefore, the isolation between them must take into consideration. The mutual coupling was less than -15dB over the whole frequency bandwidth. The proposed sensing antenna covers a wide range frequency bands from ranging 2 to 5GHz. Whilst, the communication antenna operates at 2.8GHz. The whole antenna system was designed, fabricated, and measured. Measurement and simulation results are in good agreement, which prove the proposed structure.

Key-Words: - Cognitive radio; UWB; microstrip antenna; coplanar waveguide; sensing antenna.

1 Introduction

Nowadays, the exponential growth in terms of wireless users and bandwidth-hungry applications and services, such as video conferencing and video streaming, introduces a significant issue for wireless communication systems. Given that all radio-frequency (RF) resources are already allocated by the Federal Communications Commission (FCC). Nevertheless, according to a recent measurements done by the FCC [1], the usage of spectrum is inefficient which provides a lot of spectrum holes, known as white spaces. These measures show, in fact, that a very important parts of spectrum remains underutilized or unused for 90% of time [2]. To overcome this issue, the dynamic spectrum access (DSA) technique has been proposed by the FCC [3]. The DSA technique can be considered as a wise solution to overcome the spectrum scarcity. It consists of exploiting the existing RF spectrum in an opportunistic manner, in order to detect the white spaces and then use them, so that the spectrum resources will be exploited in a more efficient way [4]. To bringing this solution to reality, many solutions have been put forth. One of the proposed solutions is the cognitive radio (CR) [5]. CR is an intelligent system which is able of continuously supervise the spectrum (sensing task), in order to detect the white spaces. When the CR system detect the free available frequency bands, it tunes dynamically its parameters to communicate within these unused frequency bands (communication task). Thus, the RF front-end of such system must ensure its main functionalities. Which are the sensing and communication tasks. To ensure the sensing task, the antenna must operate over a wide range of frequency bands, in order to cover almost all spectrum bands as possible. Although, to ensure communication task, the antenna must behave as a narrowband antenna, in order to focus power at the desired channel bandwidth. According to literature, the antennas used in CR applications can be divided into two categories [7], the one and two-port structures. The first category consists of using one antenna that can be act as an UWB or narrowband, depending on the requested task [8]-[10]. While, the second category consists of using an antenna system which contains two antennas [11]-[13], one for sensing and the other for the communication task. The second category exhibits good performances in terms of the independence of each task, because it can provide simultaneously the sensing and communication tasks. Contrariwise in the one-port structure, the two tasks cannot performed simultaneously at the same time. Nevertheless, the two-port structure provides one drawback which is the mutual coupling between the two elements. Therefore, the proposed structure must properly designed in order to get more isolation between the both antennas.

All papers presenting the integration of narrowband/UWB antennas have been recently reported in literature. In [14], an UWB disk monopole antenna and narrowband antenna designed on each side of substrate has been presented. To enhance the isolation between them, a microstrip open-loop resonator was used in order to introduce a band-stop characteristic. The narrowband antenna uses the disk monopole as a ground plane. As well for [15], the authors introduce a two-port antenna system that integrates two antennas, each one designed on a side of substrate. In order to get the narrowband response, two slots are used to act as a band-pass filter to suppress frequencies outside the desired band. The narrowband antenna operates between 5 and 6GHz. While, the UWB antenna covers from 3.5~8GHz. The one-side antenna design, was presented in [16]. The UWB and narrowband antennas were designed on the top side of substrate. The UWB antenna covers the spectrum from 3.1~11GHz. Whilst, the narrowband response was performed by two reconfigurable triangular-shaped elements. By rotating them, the narrowband antenna operates at 5.3~9.15GHz (position 1), and 3.4~4.85GHz (position 2). However, this design need to be rotatable controlled by a field-programmable gate array (FPGA), which makes it very expensive.

In this paper, an antenna system which can be suitable for RF front-end of cognitive radio systems is designed, simulated, fabricated, and measured. The antenna structure was designed on a single and cheap FR4 substrate, with an overall size of 100x65x1.58mm^3. The antenna structure consists of two antennas fed by a coplanar waveguide (CPW) lines, and designed on each side of substrate, as shown in Fig.1, in order to get more isolation between them. The sensing task was performed by the UWB antenna which covers a wide range of frequency bands from 2~5GHz. While, the communication task was ensured by the means of a narrowband antenna which can operate at 2.8GHz. A good isolation has been achieved between the two antennas, which is better than 15dB in the whole frequency band. A prototype of the proposed antenna structure was fabricated and measured. The comparison between the simulated and measured results shows good agreement, which prove the feasibility of the structure to be integrated into the RF front-end CR systems.

2 Antenna System Geometry

The configuration of the proposed antenna system is shown in Fig. 1. The two antennas and its ground plane were designed on the top side of a 1.58mm thick FR4 substrate with dielectric constant $\mathcal{E}_r = 4.3$ and loss tangent φ=0.02, the total space occupied by the entire system is 100x65x1.58mm^3. The reason behind the choice of the substrate is the low-cost, low-loss and their availability in the market. As mentioned above, the sensing and communication tasks, were performed by the means of the UWB and narrowband antennas, respectively, and were fed by two CPW lines, as shown hereafter. The CPW technology has been chosen among other technologies, due, in fact, to two reasons. Firstly, to create the ground plane on the top side of substrate, in order to get less mutual coupling between the two antennas. And in the other hand, given that as future work the design will incorporate active and passive components, the CPW technology makes the integration of electronic components very easier than the microstrip technology, since it prevents the costly and inductive via holes [17].

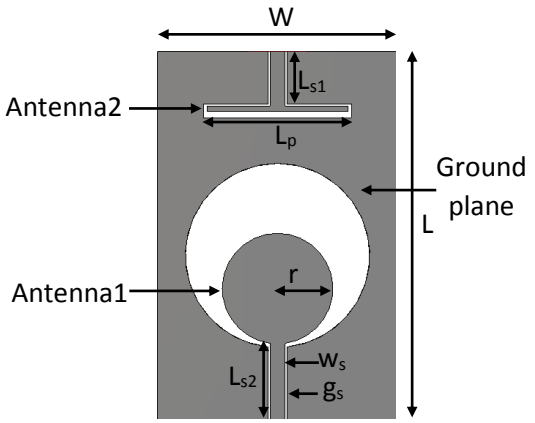

Fig. 1. Structure of the proposed antenna system.

As aforementioned, both antennas were fed by CPW technology. In order to get 50Ω input impedance, the dimensions of the feed line width as well as the two gaps were calculated using equations mentioned hereafter [17].

$$Z_{in} = \frac{30\pi}{\sqrt{\mathcal{E}_{eff,t}}} \times \frac{K(K'_t)}{K(K_t)} \quad (1)$$

$$\mathcal{E}_{eff,t} = \mathcal{E}_{eff} - \frac{\mathcal{E}_{eff}-1}{\frac{g}{0.7\times t}\times\frac{K(K)}{K\prime(K)}+1} \quad (2)$$

$$\mathcal{E}_{eff} = 1 + \frac{\mathcal{E}_r-1}{2} \times \frac{K(K\prime)\times K(K_1)}{K(K)\times K(K_1\prime)} \quad (3)$$

$$K_t = \frac{w_t}{s_t}\ ;\ K = \frac{w}{s}\ ;\ s = w + 2\times g$$

$$K_1 = \frac{\sinh\left(\frac{\pi w_t}{4h}\right)}{\sinh\left(\frac{\pi s_t}{4h}\right)} \quad (4)$$

$$K'_t = \sqrt{1-K_t^2}\ ;\ K' = \sqrt{1-K^2}\ ;\ K'_1 = \sqrt{1-K_1^2}$$

$$w_t = w + \frac{1.25\times t}{\pi} \times \left[1 + \ln\left(\frac{4\times\pi\times w}{t}\right)\right] \quad (5)$$

$$s_t = s - \frac{1.25\times t}{\pi} \times \left[1 + \ln\left(\frac{4\times\pi\times w}{t}\right)\right] \quad (6)$$

Where w, g, h, $\mathcal{E}_r$, and t, are the feed line width, the gap, substrate height, the permittivity, and the metal thickness, respectively. K(K) and K'(K) represent the complete elliptic integral of the first kind and its complement.

By using these equations and those mentioned in [18], the dimensions of the narrowband antennas were carefully calculated, in order to operate at the desired frequency. The gaps between the antenna and the ground plane were optimized by the means of the electromagnetic (EM) simulation software CST Studio Suite. The real and imaginary parts of the input impedance were presented in Fig. 2. It can be clearly observed that the real part presents different values of 50Ω at different frequencies. Since the imaginary part of the impedance represents power that is stored in the antenna near-field, which is non-radiated power, thus it must be canceled. The only frequency that provides 50Ω impedance (zero impedance) is 2.8GHz, which verifies the good matching around this frequency, as we can concluded from measurement.

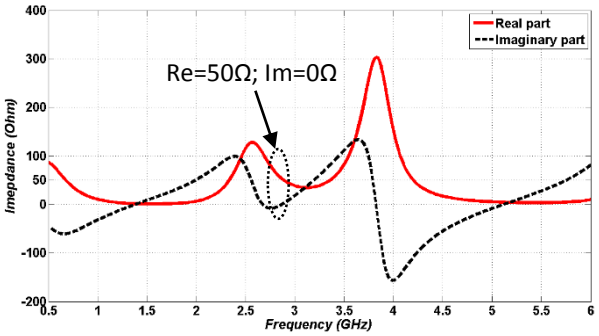

Fig. 2. The real and imaginary parts of the narrowband antenna impedance.

For the UWB sensing antenna, the width and the gaps dimensions were also calculated using equations mentioned before. While, the radius of the circular disc was calculated by the means of the equations mentioned hereafter [18].

$$\boldsymbol{r = \frac{F}{\left\{1+\frac{2\times h}{\pi\times\varepsilon_r\times F}\left[\ln\left(\frac{\pi\times F}{2\times h}\right)+1.7726\right]\right\}^{1/2}}} \quad (7)$$

$$\boldsymbol{F = \frac{8.791\times 10^9}{f_r\times\sqrt{\varepsilon_r}}} \quad (8)$$

As we can see from Fig.1, the two antennas were separated by the ground plane, and this in order to get more isolation between the two elements. Their dimensions are given in Table 1.

Table 1. The antenna system dimensions (in mm).

L	W	W_s	g_s	r	L_{s1}	L_{s2}	L_p
100	65	4	0.5	15	14	20	40

3 Measured and Simulated Results.

The antenna system was simulated using CST Studio Suite. The prototype of the structure was fabricated and tested for scattering parameters using an Anritsu Vector Network Analyzer model # MS2028C at Antenna and Microwave Lab at INPT. A photograph of the fabricated prototype is depicted in Fig.3.

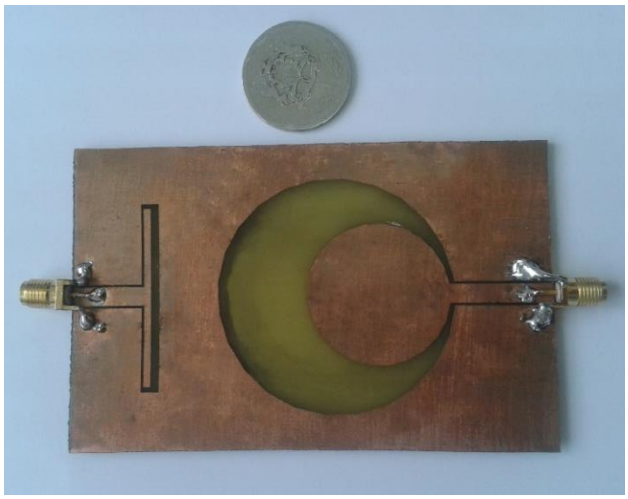

Fig. 3. Photograph of the fabricated prototype.

The proposed UWB sensing antenna covers large frequency bands ranging from 2 to 5GHz, which is 85.71% around the center frequency 3.5GHz. The simulated and measured reflection coefficient for the UWB are compared in Fig. 4. The measurement results are in close agreement with the simulated ones. The discrepancy between the two results may be explained by the inevitable proximity of SMA connector to the feed line and the slot of the CPW, and also may be due to the tolerance in manufacturing. It is clear, from Fig. 4, that around 1.5GHz, a resonant frequency was appeared. And this can be caused by the capacitive and inductive effects, which are might achieved by the small gap between the feed line and the ground plane, and also by the edge effects.

The narrowband communication antenna operates at 2.8GHz. As shown in Fig. 5, the measured and simulated reflection coefficient show that we obtain a narrow bandwidth and good matching around the desired frequency, 2.8GHz, which are about 400MHz and -35dB, respectively. The measured and simulated results show, in fact, a very good agreement, thus verifying the proposed structure. However, a small

discrepancy was observed at higher frequencies, which is due to parasitic capacitance created across the gap sides.

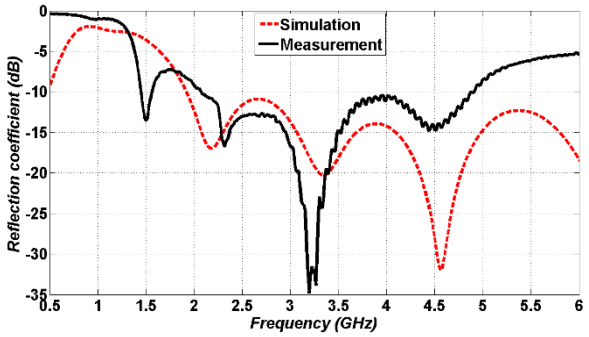

Fig. 4. Simulated and measured reflection coefficient for the UWB sensing antenna.

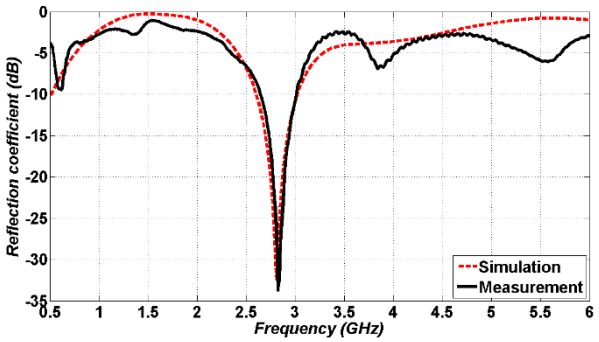

Fig. 5. Simulated and measured reflection coefficient for the narrowband antenna

Since both antennas were designed on the same side of substrate. Therefore, we must take it into account the isolation, which is a very required feature. In order to measure the coupling between the two antennas, the transmission coefficient is measured. Fig. 6 depicts the isolation between the UWB sensing and narrowband antennas. As we can see from the measurement and simulation results, the isolation is better than 15dB throughout the whole frequency bandwidth. Which exhibits a good isolation and low mutual coupling between the two elements.

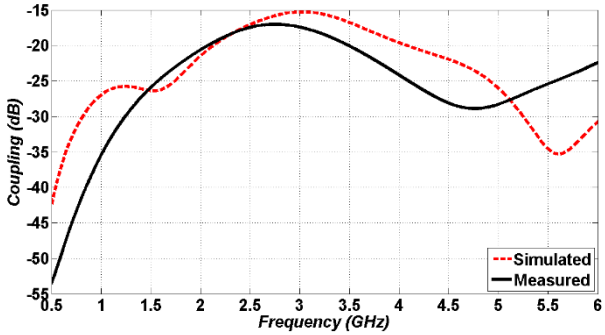

Fig. 6. Simulated and measured transmission coefficient for the narrowband antenna

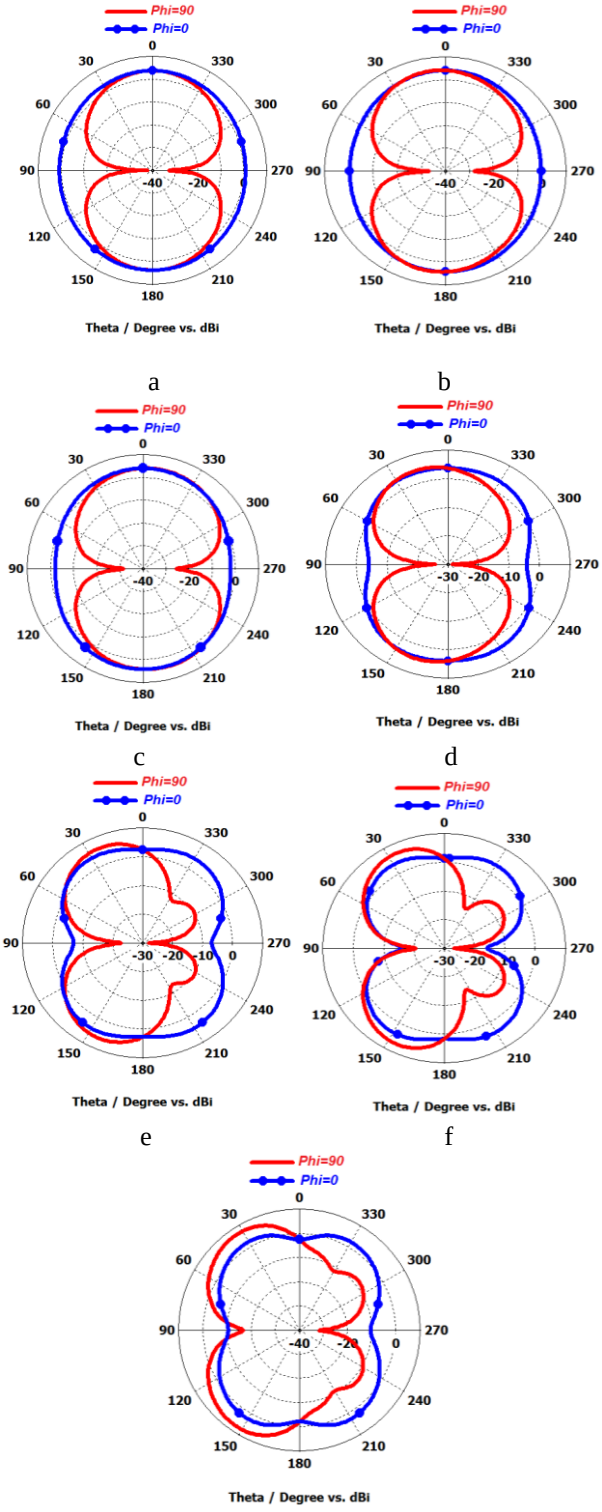

Fig. 7. Radiation patterns for UWB sensing antenna at (a) 2GHz, (b) 2.5Ghz, (c) 3GHz, (d) 3.5GHz, (e) 4GHz, (f) 4.5GHz, and (g) 5GHz. Solid: xz plane (Phi=0); circle: yz plane (Phi=90).

As aforementioned, the sensing task requires a wide bandwidth antenna to cover different frequency bands. But another basic required feature of the sensing task is the omnidirectional radiation pattern; in order to scan the environment in terms of space (geographic location) and RF spectrum by covering different angles. The computed 2-D gain patterns of the UWB sensing antenna in the yz and xz planes at different frequencies are presented in Fig. 7. At all these frequencies, the sensing antenna presents a quasi-omnidirectional feature. The peak gain at 2.5GHz, 3.5GHz, 4.5GHz, and 5GHz are 4.22dBi, 4.59dBi, 6.83dBi, and 7.38dBi, respectively.

The UWB sensing antenna exhibits the same characteristics as the printed circular monopole antennas, which is the quasi-omnidirectional radiation pattern. Nevertheless, in the yz plane (φ=90º) an asymmetric with respect to x-axis is noteworthy. As we can see, the level of radiation is lower at θ=-90º compared to θ=90º. And this can be explained simply by the localization of the narrowband antenna in this direction, which significantly affects the UWB behavior. However, the radiation patterns at different frequencies satisfy the omnidirectional feature. On the other side, the computed radiation patterns of the narrowband antenna at its resonant frequency in the xz and yz planes, are shown in Fig. 8. These patterns were taken at the operating frequency, 2.8GHz. The peak gain is about 6.05dBi, which is greater than the UWB antenna ones.

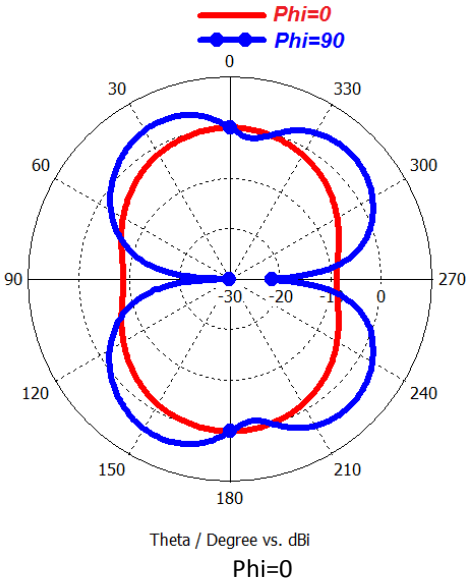

Fig. 8. Radiation patterns for narrowband antenna at 2.8GHz, in xz cut (Phi=0) and yz cut (Phi=90).

4 Conclusion

In this paper, a simple and new antenna system for cognitive radio front-end is presented. It consists of two antennas. The first one is a quasi-omnidirectional ultra-wideband antenna for spectrum sensing. The UWB sensing antenna covers large frequency bands from 2~5GHz. The second one is a narrowband dipole antenna responsible for communication at the desired frequency, 2.8GHz. Both antennas were designed on the same side of cheap FR4 substrate, to get more compactness. In order to prove the feasibility of the proposed structure, a prototype antenna was fabricated. A mutual coupling of less than -15dB was achieved over the whole bandwidth. The good agreement between simulated and measured results show, in fact, that the proposed antenna system is a best candidate to be integrated into the RF front-ends for cognitive radio systems. Table 2, summarizes the performances of the fabricated proposed antenna system.

As future work, one can integrate a passive and active components into the narrowband antenna, in order to achieve the frequency reconfigurability in such way to get the antenna operates at different frequencies.

Table 2. Antenna system performances

	Bandwidth (GHz)	Center frequency (GHz)	Peak gain (dBi)
UWB Sensing Antenna	3	3.5	4.1
Narrowband Antenna	0.4	2.8	6

Acknowledgement

The authors are grateful to Departamento de Ingenieria de Comunicaciones (DICOM), University of Cantabria (UNICAN), Spain, for support with regard to simulation software and facilities.

References:

[1] Federal Communications Commission Spectrum Policy Task Force, *Report of the Spectrum Efficiency Working Group*, November 2002.

[2] Federal Communications Commission, *Facilitating Opportunities for Flexible, Efficient and Reliable Spectrum Use Employing Cognitive Radio Technologies*, notice of

proposed rulemaking and order, FCC 03-322, December 2003.

[3] N. Kaabouch and W.-C. Hu, *Handbook of Research on Software-Defined and Cognitive Radio Technologies for Dynamic*, University of North Dakota, US Spectrum Management. 2014.

[4] Qing Zhao, Brian M. Sadler, A survey of dynamic Spectrum Access, *IEEE Signal Processing Magazine*, May 2007, pp. 79-89.

[5] Lars Berlemann, Stefan Mangold, *Cognitive Radio and Dynamic Spectrum Access*, John Wiley & Sons, Inc., 2009.

[6] J. Mitola and G. Q. Maguire, Cognitive radios: Making Software Radios More Personal, *IEEE Personal Communications*, Vol. 6, No. 4, 1999, pp. 13-18.

[7] Mohammed Al-Husseini, Karim Y. Kabalan, Ali El-Hajj and Christos G. Christodoulou, Reconfigurable microstrip antennas for cognitive radio, *Advancement in Microstrip Antennas with Recent Applications*, Prof. Ahmed Kishk (Ed.), chapter 14, InTech, 2013, pp. 337–362.

[8] Hamza Nachouane, Abdellah Najid, Abdelwahed Tribak, Fatima Riouch, Reconfigurable Antenna Combining Sensing and Communication Tasks for Cognitive Radio Applications, *Proc. of Mediterranean Conf. on Information and Communication Technologies,* May 7-9, Saidia, Morocco, 2015.

[9] Pei-Yuan Qin, Feng Wei, Y. Jay Guo, A Wideband to Narrowband Tunable Antenna Using A Reconfigurable Filter, *IEEE Transactions on Antennas and Propagation*, vol.63, no.5, May 2015, pp.2282-2285.

[10] Hamid, M.R.; Gardner, P.; Hall, P.S.; Ghanem, F., Switched-Band Vivaldi Antenna, *IEEE Transactions on Antennas and Propagation*, vol.59, no.5, May 2011, pp.1472-1480.

[11] Hussain, R.; Sharawi, M.S., A Cognitive Radio Reconfigurable MIMO and Sensing Antenna System, *IEEE Antennas and Wireless Propagation Letters*, vol.14, no., 2015, pp.257-260.

[12] E. Ebrahimi, P. S. Hall, Integrated wide-narrowband antenna for multiband applications, Microwave and Optical Technology Letters, vol. 52,no. 2, Feb. 2010, pp. 425-430.

[13] Tawk, Y.; Costantine, J.; Christodoulou, C.G., A rotatable reconfigurable antenna for cognitive radio applications, *IEEE Radio and Wireless Symposium (RWS),* vol., no., 16-19 Jan. 2011, pp.158-161.

[14] J.R. Kelly, P.S. Hall, P. Gardner, F. Ghanem, Integrated narrow/band-notched UWB, *Electronics Letters*, vol. 46, no. 12, 2010, pp. 814 - 816.

[15] F. Ghanem, P.S. Hall, J.R. Kelly, Two port frequency reconfigurable antenna for cognitive radios, *Electronics Letters*, vol. 45, no. 11, 2009, pp. 534 - 536.

[16] Y. Tawk, C.G. Christodoulou, A new reconfigurable antenna design for cognitive radio, *IEEE Antenna and Wireless Propagation Letters*, vol. 8, 2009, pp. 1378-1381.

[17] R. N. Simon, *Coplanar Waveguide Circuits Components and Systems*, John Wiley & Sons, New York, 2001.

[18] Balanis, C. A., *Antenna Theory Analysis and Design*, 3rd edition, John Wiley & Sons, Hoboken, New Jersey, 2005.